African Journal of Biological Sciences

Molecular docking-based in silico evaluation of punicic acid as a potential inhibitor of respiratory influenza viruses, including SARS-CoV-1 and SARS-CoV-2

Correspondingauthor Aarati RSupekar –

Email: aarti.supekar@gmail.com
DepartmentofPharmacognosy,Dr.DYPatilUnitechSociety'sDr.D.Y.Patil Institute ofPharmaceutical Sciences and Research, Pimpri, PunePhonenumber- 91-9623310570

Dr. SantoshSBhujbal
Email: santosh.bhujbal@dypvp.edu.in
Department of Pharmacognosy, Dr. D Y PatilUnitech Society'sDr. D. Y. PatilInstituteofPharmaceuticalSciencesandResearch,Pimpri,Pune

RashmiCYadav
Email: jrashmi18@gmail.com
Department of Pharmacognosy, Dr. D Y PatilUnitech Society'sDr. D. Y. PatilInstituteofPharmaceuticalSciencesandResearch,Pimpri,Pune

Abstract:

Emerging trends in migration, urbanisation, and worldwide travel have rendered viral epidemics a serious hazard to human health. Viral infections are a major issue due to their intricate nature, diversity, and the scarcity of vaccinations and antiviral medicines. This often leads to epidemics and pandemics. By using a computational method, this work aims to aid in the creation of efficient treatment plans by examining the mechanisms pertaining to the binding and subsequent inhibition of different respiratory influenza viruses, including SARS-CoV-2 and SARS-CoV-1 targets.Different computer screening techniques, such as the docking process, ligand-based similarity searches, or pharmacophore-based screening, are used to filter large virtual compound libraries, lowering the number of candidate compounds to a more manageable number that is subsequently physiologically verified. The drug discovery process becomes more goal-oriented thanks to this rational method, which also conserves time and money.

There are limited licenced treatments for respiratory influenza viruses including SARS-CoV-2 and SARS-CoV-1 infections, highlighting the need for more chemotherapeutic drugs to combat the disease. In this study in silico research offers an overview of the potential antiviral profiles of punicic acid against respiratory influenza viruses. As a result, it paved the path for the development of promising next-generation antiviral medications to combat respiratory influenza viruses.This study contributes to the development of effective treatment strategies through a computational approach, investigating the mechanisms in relation to the binding and subsequent inhibition of ATP-bound state of BiP (5E84), main protease (Mpro) (6LU7), spike receptor binding domain (6LZG), RNA-dependent RNA polymerase (6M71), spike glycoprotein (6VSB), NSP15 endonuclease (6VWW), Nsp9 RNA-binding protein (6W4B), papainlike protease (6W9C), and neurominadase fromH1N1 (5NZ4)the antiviral inhibitory effects of naturally occurring compounds punic acid was examined and compared with standard. Our comprehensive computational and statistical study indicates that the phytochemicals such as punicic acid can be used to design potential broadantiviral inhibitors against respiratory influenza viruses including SARS-CoV-2 and SARS-CoV-1.

Keywords: respiratory influenza viruses, SARS-CoV-2, SARS-CoV-1, Punic acid, molecular

Introduction:

Respiratory influenza viruses including SARS-CoV-2 and SARS-CoV-1 is a fatal virus that causes the illness and spreads to people when they come into contact with infected people or animals.With the exponential growth of respiratory viral diseases, SARS-CoV-1 and SARS-CoV-2, there is an increasing demand for medications to treat these infections.Currently, no effective drug has been developed; however, several studies are being conducted around the world. Despite the fact that SARS-CoV-2 has a high infection rate, there are no reliable treatment approaches available to address the illness (1).On-going scientific endeavours are focused on discovering antiviral medicinesfor respiratory influenza viruses, including SARS-CoV-2 and SARS-CoV-1.An alternative method for discovering an efficient cure is repurposing drugs, which entails examining existing pharmacological molecules for their potential as antiviral medicines against respiratory influenza viruses such as SARS-CoV-2 and SARS-CoV-1. Leading pharmaceutical companies and research institutions have employed computer-aided drug discovery (CADD) techniques in preliminary studies that aim to speed up the process of drug discovery and development, thereby decreasing costs and failures in the final stage.As a result of recent developments in robotics, high-throughput screening using microfluidic systems may now be automated, which opens the door to the possibility of drug repurposing. There are a number of computational drug repurposing techniques available; the three main types of computational drug repositioning methods utilised are network-based designs, structure-based methods, and artificially intelligent (AI) methods used to discover novel drug-target relationships beneficial for new therapies.Repurposing of FDA-approved medications has been emphasised in numerous research to identify possible inhibitors utilising structure-based drug design studies(2).

Punicic acid, the major bioactive component of pomegranate (Punicagranatum) seed oil, is an omega-5 isomer of conjugated α-linoleic acid. It has powerful anti-oxidative and anti-inflammatory actions, which contribute to its favourable effect against a wide range of disorders. Punicic acid lowers oxidative damage and inflammation by boosting the expression of peroxisome proliferator-activated receptors.aIn light of the foregoing factors, we conducted a study to assess the anti-viral potential of physiologically active phytochemicals present in traditional medicines (Ayurvedic medicines, Chinese medicines, etc.) with potential inhibitory properties against the virus. Because the treatment was based on empirical findings, we chose to screen and identify the important bioactive components from plants that were already known to have immunomodulatory effects, such as liquorice, tulasi, and pomegranate, as well as plants that are used as rasayana medicines in Ayurveda (3).

1.0)   **Material and methods:**

1.1)   **Retrieving Herbal Compounds and Preparation of Drug Library**

The 3D structures of glycyrrhezinic acid from liquorice were retrieved from PubChem database. Compounds with missing.mol/.sdf files were drawn and converted with the help of the Structure File Generator (https://cactus.nci.nih.gov/translate/) and Online SMILES Translator.

1.2)   **Target Protein Retrieval and Preparation**

On the basis of literature survey, we found that various targets, such as the ATP-bound state of BiP (5E84), main protease (Mpro) (6LU7), spike receptor binding domain (6LZG), RNA-dependent RNA polymerase (6M71), spike glycoprotein (6VSB), NSP15 endonuclease (6VWW), Nsp9 RNA-binding protein (6W4B), papainlike protease (6W9C), and neurominadase from H1N1 (5NZ4) are major target to study antiviral activity against respiratory influenza viruses including SARS-CoV-1 and SARS-CoV-2. Therefore, the fasta sequence of the above-mentioned various targets for antiviral activity against respiratory influenza viruses, including SARS-CoV-1 and SARS-CoV-2, was retrieved from the National Centre for Biotechnology information server as well as searched resembling biological sequences available on Protein Data Bank using the Basic Local Alignment Search tool (BLAST), where we sorted the top 5 to 10 selected sequences for their better
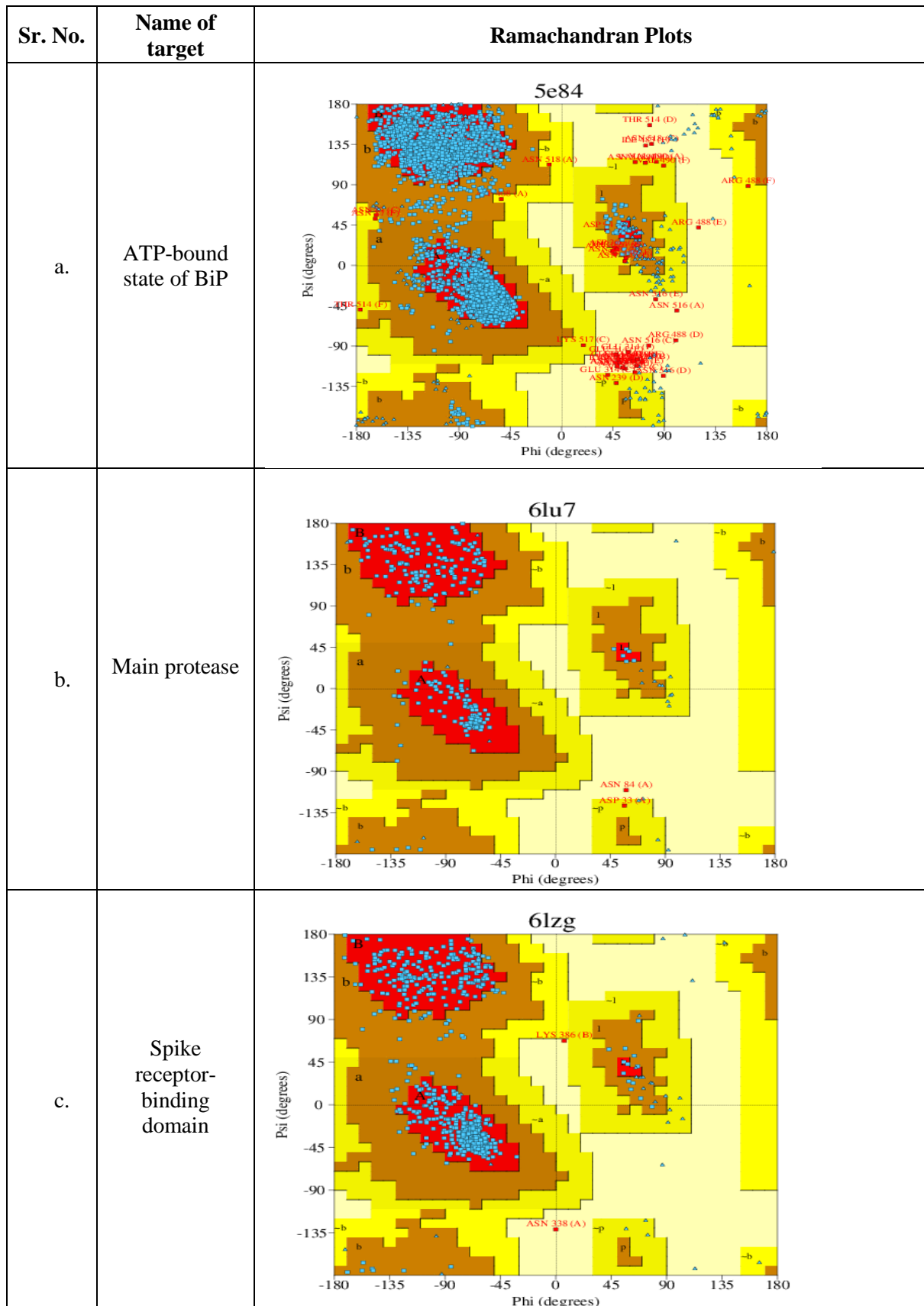
query coverage, percentage identity, and E-value. The PDB databank was used to obtain the three-dimensional X-Ray crystallographic structure of various targets, including the ATP-bound state of BiP (5E84), main protease (Mpro) (6LU7), spike receptor binding domain (6LZG), RNA-dependent RNA polymerase (6M71), spike glycoprotein (6VSB), NSP15 endonuclease (6VWW), Nsp9 RNA-binding protein (6W4B), papainlike protease (6W9C), and neurominadase from H1N1 (5NZ4). The accession number of each target was validated using parameters such as resolution, Mutation, wwPDB Validation, co-crystal ligand, and Ramachandran plot.
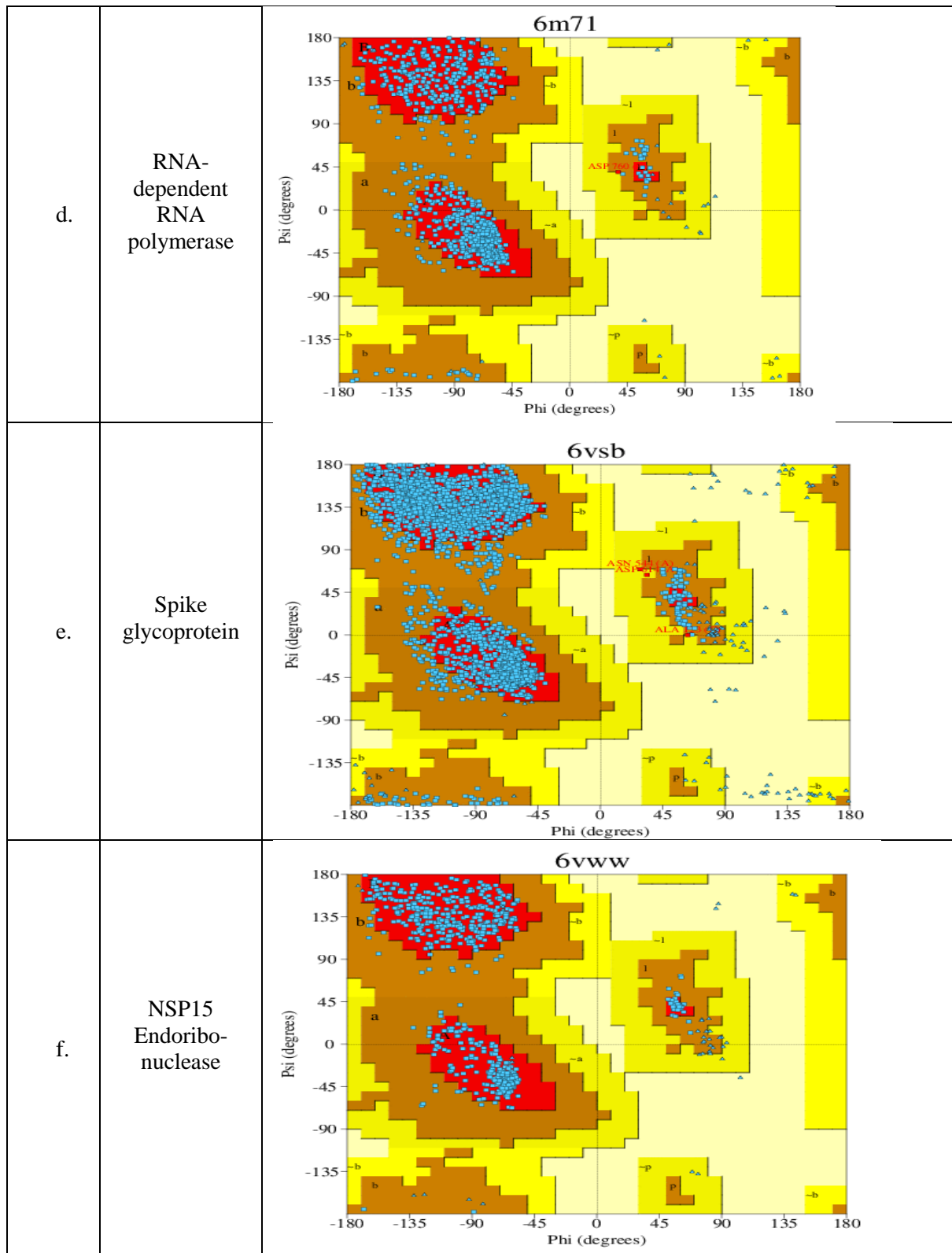
Table 1 compared standard values and recovered protein to validate docking study protein.

Parameters	Protein Details									Standards
Targets	ATP-bound state of BiP	Main protease	Spike receptor-binding domain	RNA-dependent RNA polymerase	Spike glycoprotein	NSP15 Endoribo-nuclease	Nsp9 RNA binding protein	Papain-like protease	Neuraminidase from H1N1	-
Protein Id	5E84	6LU7	6LZG	6M71	6VSB	6VWW	6W4B	6W9C	5NZ4	-
Method of Experiment	X-RAY Diffraction									
Mutation	No	No	No	No	No	No	No	No	No	No
Resolution	2.99A^0	2.16A^0	2.50A^0	2.90A^0	3.46A^0	2.20A^0	2.95A^0	2.70A^0	1.36 Å	Near about 2.00A^0
wwPDB Validation	Better	Better	Better	Better	Better	Better	Better	Better	Better	Better
Ramchandran Plot (by PROCHECK server) Residues in favoured + Allowed regions	89.8%	90.6%	90.8%	87.2%	84.0%	93.1%	91.1%	86.1%	100%	>80 %

Table 1: Comparison between standard values and retrieved protein for validation of protein Selected for docking study.

The angles from a Ramachandran plot can be used to verify the solution to a crystal structure as well as determining the role of an amino acid in secondary structure. It also helps with constraining structure prediction simulations and defining energy functions. It shows the regions in protein structure that are energetically permitted for backbone dihedral angles ψ against φ of amino acid residues. The below table 2 shows Ramachandran Plots for several study targets. The three-dimensional geometry of the protein model was determined using the PROCHECK web tool, which calculated the Ramachandran plot and generated results for residues in various coloured regions, namely red (favoured), yellow (additionally allowed), pale yellow (generously allowed), and whitish yellow (disallowed).

Sr. No.	Name of target	Ramachandran Plots
a.	ATP-bound state of BiP	
b.	Main protease	
c.	Spike receptor-binding domain	

d.	RNA-dependent RNA polymerase	
e.	Spike glycoprotein	
f.	NSP15 Endoribo-nuclease	

g.	Papain-like protease	
h.	Papain-like protease	
i.	Neuraminidase from H1N1	
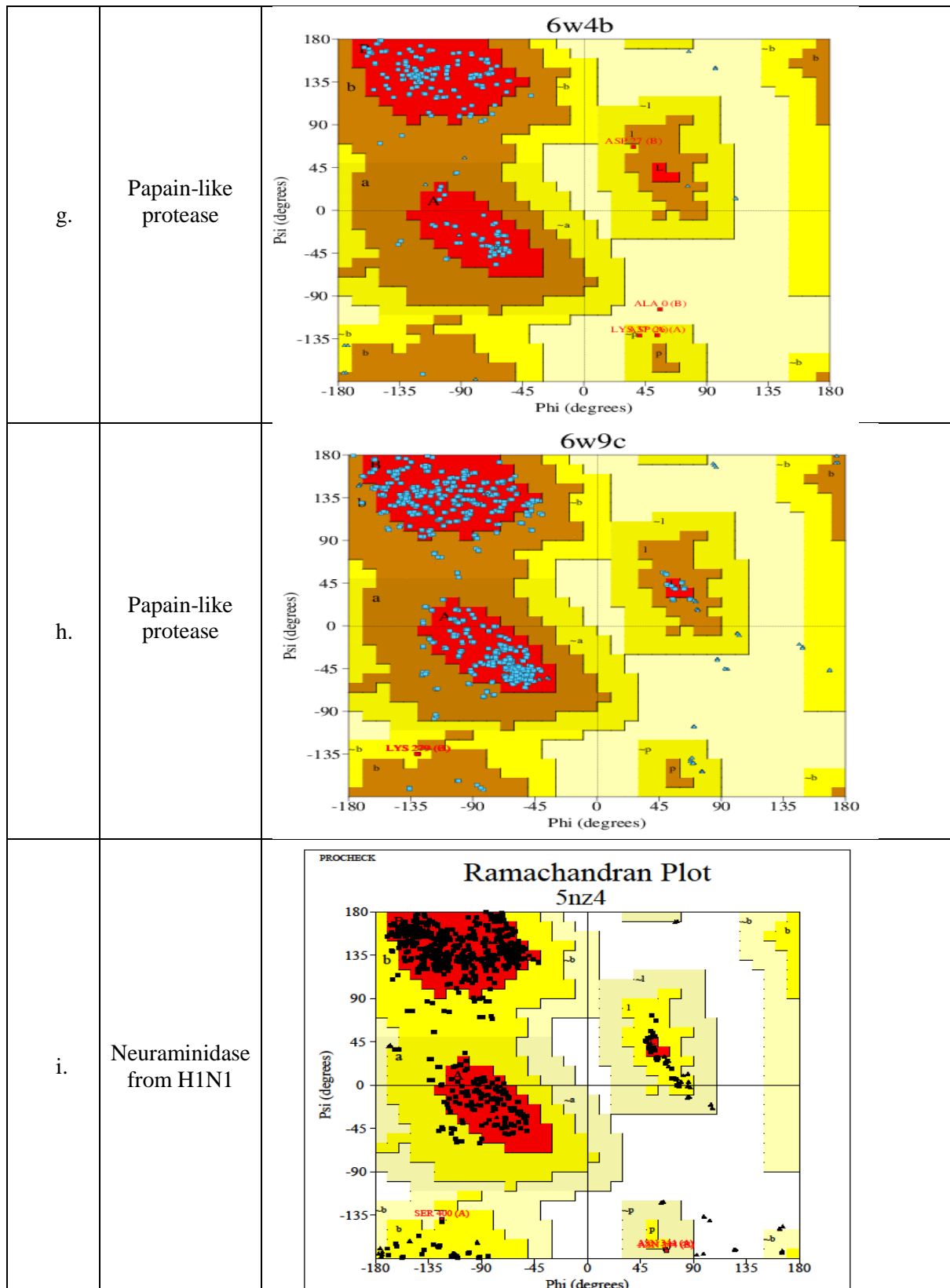
Figure 1: Ramachandran Plot of 5E84, 6LU7, 6LZG, 6M71, 6VSB, 6VWW, 6W4B, 6W9C, 5nz4 obtained from PROCHECK serve

Every molecule has the potential to be either a macromolecule or a micro-molecule, however it is necessary to optimize and minimize the latter before conducting a docking study. The protein data bank's PDB [sum server, a pictorial library of 3D structures for interactions of conventional inhibitors with protein, has been used to confirm the binding pocket. The proteins with missing

residues were completed and side chains were synthesized using CHIMAERA v1.16. Subsequently, they underwent optimization and minimization before to being included in the docking study. The optimization of proteins is achieved by configuring 1000 iterations of the Steepest Descent algorithm, with a step size of 0.1 A0, followed by 100 iterations of the Conjugate Gradient algorithm, with a size of 0.1 A0. All hydrogen atoms, including the ones with slower rates of addition, were included. Protonation statuses were assigned to the histidine residues. Additional fees were applied for both conventional (using the AMBER ff14SB force field) and unconventional (using the AM1-BCC force field) residues. The net charges of all non-standard entities were stabilized to enable the computation of their atomic partial charges using ANTECHAMBER charges. The protein was purified by removing any nonstandard residues, such as water molecules, cocrystal ligands, and superfluous chains, using Biovia Discovery Studio visualizer V21.1.0.20298 after optimization and minimization.

1.3) Grid generation

Auto-Dock Tools, Chimera, and Maestro were used for receptor grid identification. The Workspace displayed various targets, including the ATP-bound state of BiP (5E84), main protease (Mpro) (6LU7), spike receptor binding domain (6LZG), RNA-dependent RNA polymerase (6M71), spike glycoprotein (6VSB), NSP15 endonuclease (6VWW), Nsp9 RNA-binding protein (6W4B), papain like protease (6W9C), and neurominadase from H1N1 (5NZ4) protein. The grid's volume was determined by utilising the pocket's dimensions. The size of the enclosing box was minimised to ensure its compatibility with the protein's active site and the predicted ligands for docking. Computer-based target identification primarily encompasses the identification of disease-related targets, the identification of binding sites, and the evaluation of drug ability. The ability of the ligand and target protein to interact can be ascertained using the binding site. The problem of low utility or druggability commonly encountered in clinical trials can be effectively mitigated through early druggability assessment of proteins. Moreover, it is necessary to ascertain whether the targeted protein is suitable for therapeutic purposes. The discovery of binding sites and assessment of druggability are necessary for protein function annotation, elucidating cellular activity mechanisms, conducting molecular docking, and designing rational drugs. The below table 3 shows active site for binding and grid generation

Protein	Active Sites Amino Acids
5E84	GLU201,ASP224,GLY226,GLY227,GLY228,ALA229,GLY255,GLU256,GLU293,LYS296,ARG297,ASP34,GLY36,GLY363,GLY364,SER365,THR37,THR38,TYR39,ASP391,VAL394,SER40,CYS41,ILE61,LYS96
6LU7	PHE140,LEU141,ASN142,GLY143,SER144,CYS145,HIS163,GLU166,THR25,THR26,LEU27,HIS41,MET49,VAL3,LEU4
6LZG	HIS345,PRO346,THR347,ALA348,ASP350,LEU370,THR371,HIS374,GLU375,HIS378,ASP382,ARG393,ASN394,GLU398,HIS401,GLU402,GLU406,SER409,LEU410,GLN442,TYR515,ARG518
6M71	ASP452,TYR455,TYR456,THR540,MET542,LYS545,ARG553,ALA554,ARG555,THR556,ALA558,TRP617,ASP618,TYR619,LYS621,CYS622,ASP623,ARG624,GLU665,VAL667,LYS676,THR680,SER681,SER682,THR687,ALA688,ASN691,LEU758,SER759,ASP760,ASP761,ALA762,LYS798,TRP800,GLU811,CYS813,SER814
6VSB	GLN1002,TYR756,PHE970,ASP994,ARG995,THR998,GLY999,GLN1002,TYR756,PHE759,PHE970,ASP994,ARG995,THR998,GLY999,GLN1002,TYR756,PHE970,ASP994,ARG995,THR998,GLY999,ALA363
6VWW	HIS235,ASP240,HIS243,GLN245,LEU246,GLY247,HIS250,LYS290,VAL292,SER294,MET331,TRP333,GLU340,THR341,TYR343,LYS345,LEU346
6W4B	ARG100,LEU104,LEU107,ALA108,LEU113,GLU71,PRO72,CYS74,PHE76,LEU89,PHE91,ASN97,MET102,ASN3,ASN34,GLU4,LEU5,SER6,VAL8,LEU98
6W9C	CYS111,LEU162,GLY163,ASP164,ARG166,GLU167,MET208,PRO248,TYR264,ASN267,TYR268,GLY271,TYR273,THR301,ASP302,LYS105,TRP106,ALA107,ASP108

Table 2: proteins with their active site amino acid.

The size of the enclosing box was minimised to ensure its compatibility with the protein's active site and the anticipated ligands for docking.

Table 3 displays the grid parameters for active site determination.

PDB ID	CENTRE CO-ORDINATES			SIZE CO-ORDINATES		
	X	Y	Z	X	Y	Z
5E84	32.688	-14.185	-39.441	30	30	30
6LU7	-11.514	16.061	67.4	30	30	30
6LZG	-23.866	13.4	-16.44	30	30	30
6M71	227.549	226.92	238.335	30	30	30
6VSB	-48.029	34.785	29.588	30	30	30
6VWW	40.238	-12.061	18.809	40	40	40
6W4B	40.238	-12.061	18.809	30	30	30
6W9C	-37.109	8.793	32.976	40	40	40

Table No.3 Different Grid Parameter

1.4) Ligands Preparation:

The ligand molecules were created using MarvinSketch v21.13 and saved in the 3D MOL2 format. All three compounds underwent processing and optimisation using UCSF Chimaera v1.15 with the AM1-BCC semi-empirical force field. The default parameters were used, including 1000 steps of steepest descent and 100 steps of conjugate gradient.

1.5) Molecular Docking of Target Protein with Ligands:

Once the ligands and proteins were obtained, their structures were converted to the pdbqt format using an internal bash script created with AutoDock tools 1.5.6 for ligands and ADFRsuit for proteins. In this script, all of the ligands' rotatable bonds were left free to rotate, and the receptor was regarded as stiff. For docking studies, we utilised the AutoDockVina 1.2.3, with 0.375 ˚A spacing between grid points. The grid box was precisely positioned at the active site of the enzyme with great accuracy, enabling the programme to explore potential interaction sites between the ligands and the receptor. Alternative arrangements were deemed as the standard. The XYZ centre has coordinates (X*Y*Z), and the grid box has dimensions of 20 * 20 * 20 A0. The CPU parameter was set to 23, the exhaustiveness parameter was set to 32, the number of modes parameter was set to 9, and the energy range parameter was set to 3. The redockings were executed using identical settings as the previous dockings.
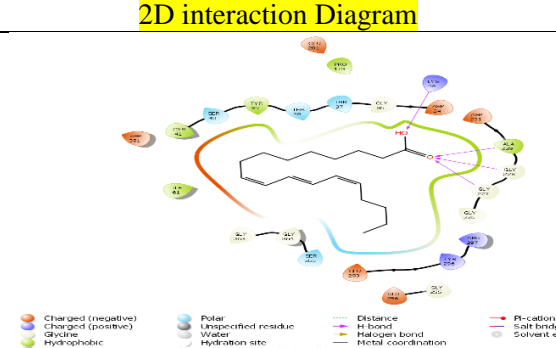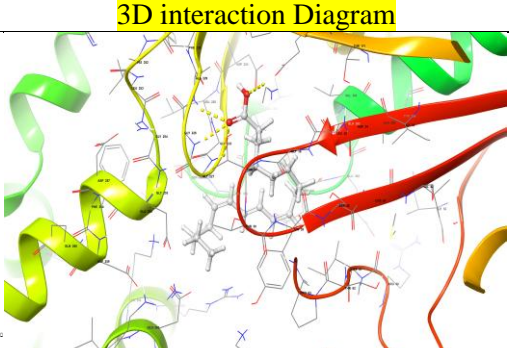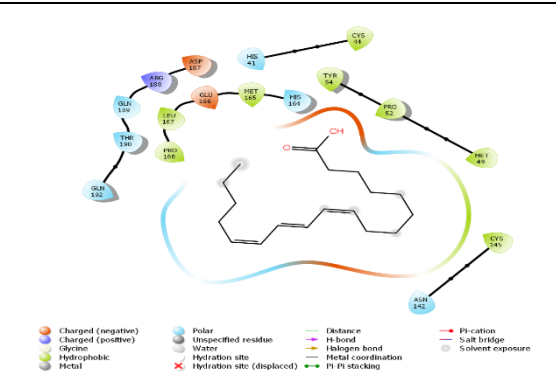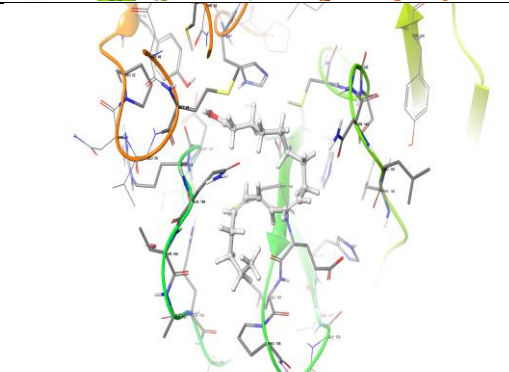
1.6) Visualization:

The results received from AutodockVina processing were used to create a complex utilising the Biovia Discovery Studio visualizer. Maestro 12.3 (academic version) and LigPlus 1.2 were

utilised to generate 2D and 3D pictures of complexes. The interactions and binding energies of the test substances were evaluated and compared to those of conventional inhibitors.

The pharmacodynamics of the chemical were investigated using adsorption, distribution, metabolism, and excretion. SWISS-ADME (http://www.swissadme.ch/) is a website that allows users to sketch their potential ligand or drug molecule and provides parameters like lipophilicity, water solubility, and drug likeness rules. Predicting chemical toxicity is a crucial aspect of medication discovery. The toxicity analysis was conducted using the pkCSM (http://biosig.unimelb.edu.au/pkcsm/prediction) and PROTOX (http://tox.charite.de/protox_II/) web servers. It predicts the level of tolerance of the small molecule when injected into human and animal models. Several toxicological consequences, such as AMES toxicity, LD50, maximal resistance dose for humans, and hepatotoxicity, are being considered.

2.0)   Result & Discussion:

We screened as punicicacid obtained from pomegranate seed oil, as well as compared it with commercially available antiviral drug called Ribavirin using in silico approach. Nine protein structures were chosen for virtual screening: ATP-bound state of BiP (5E84), main protease (Mpro) (6LU7), spike receptor binding domain (6LZG), RNA-dependent RNA polymerase (6M71), spike glycoprotein (6VSB), NSP15 endonuclease (6VWW), Nsp9 RNA-binding protein (6W4B), papainlike protease (6W9C), and neurominadase from H1N1 (5NZ4). In silico toxicity assessments confirmed that all of the chemicals were safe. The bioactivity prediction indicates that these chemicals might exert their effects by inhibiting proteases or enzymes. In order to find a substance that can potentially inhibit respiratory influenza viruses as well as SARS-CoV-1 and SARS-CoV-2, a method called structure-based molecular docking was used. This method involved testing the effectiveness of punicic acidas well as a commercially available antiviral drug called Ribavirin. This compound was chosen because they have shown therapeutic potential against various infectious diseases, including their ability to fight against malaria and viruses.

The pharmacodynamics of the chemical were investigated using adsorption, distribution, metabolism, and excretion. SWISS-ADME (http://www.swissadme.ch/) is a website that allows users to sketch their potential ligand or drug molecule and provides parameters like lipophilicity, water solubility, and drug likeness rules. Predicting chemical toxicity is a crucial aspect of medication discovery. The toxicity analysis was conducted using the PROTOX (http://tox.charite.de/protox_II/) and pkCSM (http://biosig.unimelb.edu.au/pkcsm/prediction) web servers. It predicts the level of tolerance of the small molecule when injected into human and animal models. Several toxicological consequences, such as AMES toxicity, LD50, maximal resistance dose for humans, and hepatotoxicity, are being considered. Target prediction is a valuable tool for comprehending the molecular pathways that contribute to a specific phenotypic or bioactivity. It also aids in rationalising anticipated adverse effects, forecasting target interactions, and assessing the therapeutic potential of significant drugs. Swiss target prediction is an internet-based tool that can forecast the macromolecular targets of bioactive small compounds, including proteins from humans, cats, and rats.

The 2D interaction diagram (Figure 1) described the interaction between Bioactive phytoconstituent (glycyrrhezinic acid) docked against ATP-bound state of BiP (5E84), main protease (Mpro) (6LU7), spike receptor binding domain (6LZG), RNA-dependent RNA polymerase (6M71), spike glycoprotein (6VSB), NSP15 endonuclease (6VWW), Nsp9 RNA-binding protein (6W4B), papainlike protease (6W9C), and neurominadase from H1N1 (5NZ4) respectively.

The mean docking score values, ΔG (Kcal/mol), and the likelihood of binding to the active site are displayed in the table 4.

Sr. No.	Molecule	ATP-bound state of	Main protease	Spike receptor-	RNA-dependent	Spike glycoprotein	NSP15 Endoribo-	Nsp9 RNA binding	Papain-like proteas	Neuraminidase from

		BiP		binding domain	RNA polymerase		nuclease	protein	e	H1N1
Protein Id		5E84	6LU7	6LZG	6M71	6VSB	6VWW	6W4B	6W9C	5NZ4
1	Ribavirin	-8.825	-6.61	-6.18	-6.151	-6.067	-6.921	-4.847	-5.867	-8.855
2	Punicic Acid	-6.542	-4.646	-5.766	-4.414	-6.013	-6.101	-5.847	-5.532	-7.068

Table 4: Docking Score and intermolecular interactions of ligands **ATP-bound state of BiP, Main protease, Spike receptor-binding domain, RNA-dependent RNA polymerase, Spike glycoprotein, NSP15 Endoribonuclease, Nsp9 RNA binding protein, Papain-like protease and Neuraminidase from H1N1**using LigPlot v1.4.5, PLIP server, Maestro V12.8 and Biovia Discovery studio visualizer

The docking software GOLD (version5.7.3) was used for virtual screening. The GOLD software suite's DockingWizard was used to configure the docking runs. The number of docking runs per molecule was set to 15 for each ligand. The scoring function ChemPLP was chosen as the fitness function, with default values.The default settings for the genetic algorithm parameters that dictated docking speed were applied, specifically "slow/automatic". The dependability of the molecular docking approach was initially evaluated using self-docking, which effectively recovered docking poses of the relevant ligands from the protein structures. RMSD values less than 1 Å. The docking results for all nine protein structures were assessed separately using the following criteria: the top 100 molecules rated by the Chem PLP score from the IHDB database were selected for visual examination. To analyse the MNPDB data, a specific threshold was established for each protein structure based on the Chem PLP score of the redocked ligands. The threshold was set at 80.00 for 7JN2 and 4OW0, and 70.00 for 6W63.Subsequently, all docking stances exceeding this criterion were assessed through visual examination.

Sr.No	Targets	2D interaction Diagram	3D interaction Diagram
1.	ATP-bound state of BiP (5E84)		
2.	main protease (Mpro) (6LU7)		

3.	spike receptor binding domain (6LZG)		
4.	RNA-dependent RNA polymerase (6M71)		
5.	spike glycoprotein (6VSB)		
6.	NSP15 endonuclease (6VWW)		

7.	Nsp9 RNA-binding protein (6W4B)		
8.	papainlike protease (6W9C)		
9.	neuromina dase from H1N1 (5NZ4)		
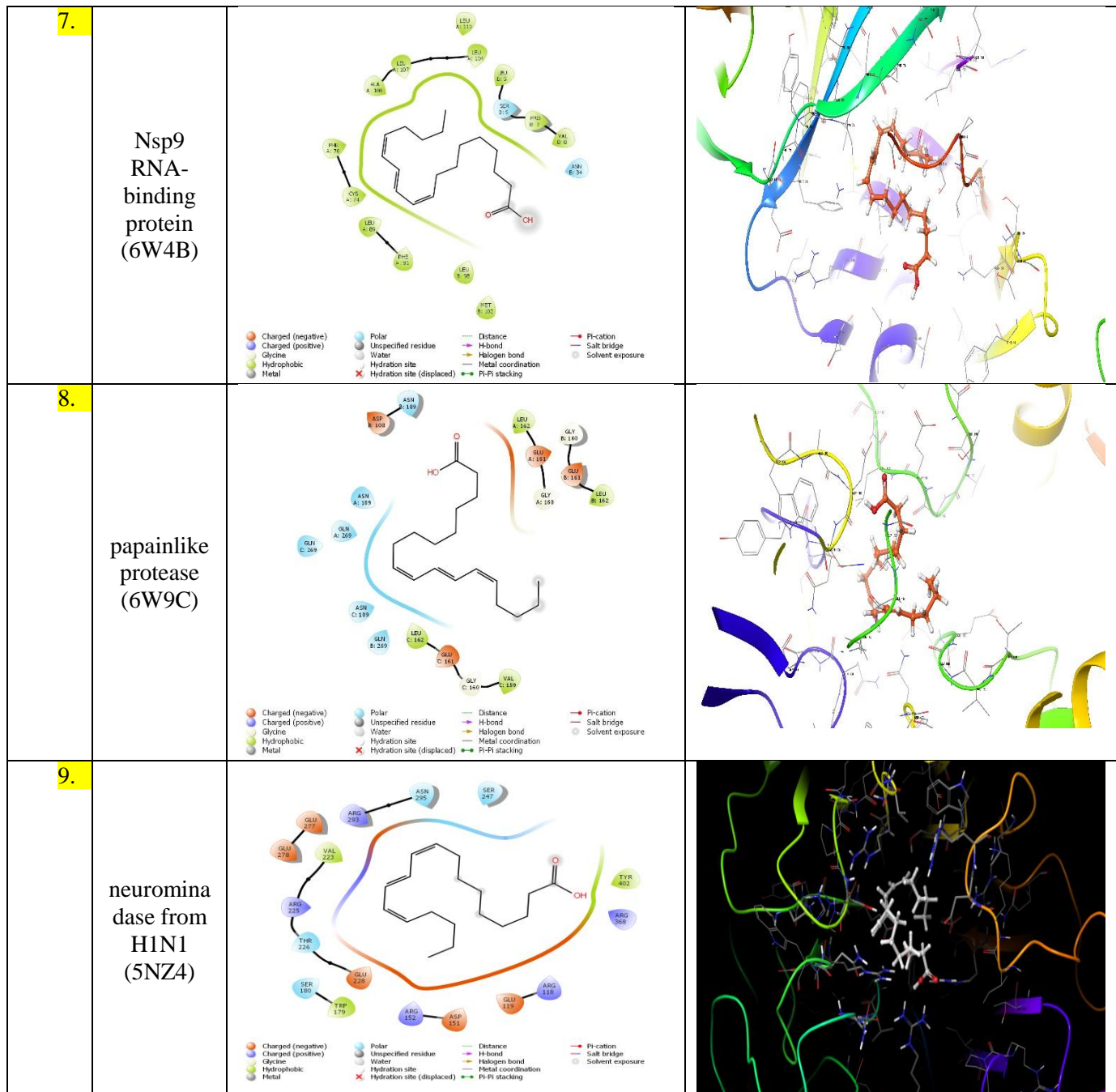
Figure 2: 2D interaction diagram 3D interaction diagram of Punicic acid with **ATP-bound state of BiP, Main protease, Spike receptor-binding domain, RNA-dependent RNA polymerase, Spike glycoprotein, NSP15 Endoribonuclease, Nsp9 RNA binding protein, Papain-like protease and Neuraminidase from H1N1.**

3.2) Target prediction:

Protein-Ligand Interaction Profiler

SR.NO	Targets	MOLECULES	BINDING ENERGY	INTERACTION	RESIDUE ID	DISTANCE A^0
1	ATP-bound state of BiP (5E84)		-6.542	Hydrophobic Interactions	LEU162A	3.54
					LEU162B	3.8
					LEU269C	3.51
					GLN269B	3.59
					GLN269C	3.71
				Hydrogen Bonds	ASP108B	3.22
					LEU162A	2.76
2	Main protease (Mpro) (6LU7)		-4.646	Hydrophobic Interactions	MET165A	3.52
					GLU166A	3.78
					PRO168A	3.87
					GLN189A	3.64
					GLN189A	3.91
				Salt Bridges	HIS41A	3.99
3	Spike receptor binding domain (6LZG)		-5.766	Hydrophobic Interactions	PHE40A	3.66
					PHE40A	3.6
					TRP69A	3.54
					LEU73A	3.72
					ASP350A	3.57
					PHE390A	3.73
					PHE390A	3.7
					LEU391A	3.71
					ARG393A	3.8
				Hydrogen Bonds	ALA348A	2.3
					ASP350A	2.11
4	RNA-dependent RNA polymerase (6M71)	**Punicic_acid**	-4.414	Hydrophobic Interactions	ASP618A	3.74
					ASP618A	3.76
					LYS798A	3.94
					GLU811A	3.95
				Hydrogen Bonds	TRP800A	2.25
5	spike glycoprotein (6VSB)		-6.013	Hydrophobic Interactions	TYR756A	3.44
					TYR756C	3.69
					PHE970B	3.77
					PHE970B	3.88
					PHE970C	3.73
					ARG995C	3.94
					THR998A	3.91
				Hydrogen Bonds	THR998B	3.71
					THR998C	2.04
					GLN1002B	3.2
6	NSP15 endonuclease (6VWW)		-6.101	Hydrophobic Interactions	LEU201B	3.83
					LEU252B	3.58
					VAL295B	3.82
					ASP297B	3.79
				Hydrogen Bonds	ASP268B	3.12
				Salt Bridges	LYS90B	5.24
					LYS277B	4.21
7	Nsp9 RNA-binding protein		-5.847	Hydrophobic Interactions	LEU5B	3.67
					VAL8B	3.7

	(6W4B)				VAL8B	3.57
					PHE76A	3.53
					PHE76A	3.57
					LEU89A	3.85
					LEU89A	3.66
					PHE91A	3.94
					LEU104A	3.1
					LEU107A	3.66
					LEU107A	3.77
					ALA108A	3.63
					LEU113A	3.68
					LEU113A	3.66
8	papainlike protease (6W9C)		-5.532	Hydrophobic Interactions	GLU161A	3.96
					LEU162A	3.55
					LEU162B	3.49
					GLN269A	3.11
					GLN269C	3.93
				Hydrogen Bonds	THR158A	2.49
					GLN269B	2.47
9	neurominadase from H1N1 (5NZ4)		-7.068	Hydrophobic Interactions	LEU113A	3.66
					GLU161A	3.96

Table 6: The interaction and distance between inhibitors and critical amino acids of nine different targets in docking complexes was assessed using the LIGPLOT software.

3.0) Conclusion:

It is determined that natural products can serve as an effective source for drugs targeting respiratory influenza viruses, including SARS-CoV-2 and SARS-CoV-1. Therefore, ursolic acid, punic acid, and Glycyrrhetinic acid have the potential to be utilised as antiviral medications against respiratory influenza viruses, including SARS-CoV-2 and SARS-CoV-1.

As a result of our findings using a structural bioinformatics approach, we believe that all of these natural drugs have the potential to be used against Respiratory influenza viruses including SARS-CoV-2 and SARS-CoV-1 and should be investigated further as Respiratory influenza viruses including SARS-CoV-2 and SARS-CoV-1 preventative therapies.

4.0) Declarations :

Author contribution statement :
All listed authors made substantial contributions to the conception and composition of this article.

Conflict of interests :
The authors have disclosed no conflicts of interest.
Reference:

1. Islam AU, Serseg T, Benarous K, Ahmmed F, Kawsar SM. Synthesis, antimicrobial activity, molecular docking and pharmacophore analysis of new propionylmannopyranosides. Journal of Molecular Structure. 2023 Jun 14:135999.

2. Abu R, Hasan MM, Aeyas A, Chowdhury FI, Khandaker MU. In-silico approach to designing effective antiviral drugs against SARS-CoV-2 and SARS-CoV-1 from reported phytochemicals: a quality improvement study. Annals of Medicine and Surgery. 2023 Jul 1;85(7):3446-60.

3. Serseg T, Benarous K, Serseg M, Rehman HM, El Bakri Y, Goumri-Said S. Discovery of inhibitors against SARS-CoV-2 associated fungal coinfections via virtual screening, ADMET evaluation, PASS, molecular docking, dynamics and pharmacophore studies. Arab Journal of Basic and Applied Sciences. 2022 Dec 12;29(1):337-50.

4. Mamedov NA, Egamberdieva D. Phytochemical constituents and pharmacological effects of licorice: a review. Plant and human health, Volume 3: Pharmacology and therapeutic uses. 2019:1-21.

5. Wahab S, Annadurai S, Abullais SS, Das G, Ahmad W, Ahmad MF, Kandasamy G, Vasudevan R, Ali MS, Amir M. Glycyrrhizaglabra (Licorice): A comprehensive review on its phytochemistry, biological activities, clinical evidence and toxicology. Plants. 2021 Dec 14;10(12):2751.

6. Chandra A, Chaudhary M, Qamar I, Singh N, Nain V. In silico identification and validation of natural antiviral compounds as potential inhibitors of SARS-CoV-2 methyltransferase. Journal of Biomolecular Structure and Dynamics. 2022 Sep 22;40(14):6534-44.

7. MadhaviSastry G, Adzhigirey M, Day T, Annabhimoju R, Sherman W. Protein and ligand preparation: parameters, protocols, and influence on virtual screening enrichments. Journal of computer-aided molecular design. 2013 Mar;27:221-34.

8. Padmika W, Uthpali M, Nimanthi J. Molecular docking and ADMET based study to identify potential phytochemical inhibitors for papain-like protease of SARS-CoV-2 (preprint).

9. Olawale F, Iwaloye O, Elekofehinti OO. Virtual screening of natural compounds as selective inhibitors of polo-like kinase-1 at C-terminal polo box and N-terminal catalytic domain. Journal of Biomolecular Structure and Dynamics. 2022 Dec 26;40(24):13606-24.

10. Pitsillou E, Liang J, Ververis K, Lim KW, Hung A, Karagiannis TC. Identification of small molecule inhibitors of the deubiquitinating activity of the SARS-CoV-2 papain-like protease: in silico molecular docking studies and in vitro enzymatic activity assay. Frontiers in chemistry. 2020 Dec 8;8:623971.

11. **Anggiresti, Kinasih.,Alim, El, Hakim., Dyah, Ayu, Puspita, Arum., Aulia, Noor, Ramadhani., Endang, Semiarti. In Silico Study of Secondary Metabolites in Dendrobium spp. as SARS-CoV-2 Antivirus on Main Protease (Mpro). JurnalRisetBiologidanAplikasinya, (2022).;4(1):19-25. doi: 10.26740/jrba.v4n1.p19-25**

12. Pandit M, Latha N. In silico studies reveal potential antiviral activity of phytochemicals from medicinal plants for the treatment of COVID-19 infection. Research Square; 2020. DOI: 10.21203/rs.3.rs-22687/v1.

13. Mishra A, Pathak Y, Choudhir G, Kumar A, Mishra SK, Tripathi V. Natural compounds as potential inhibitors of novel coronavirus (COVID-19) main protease: An in silico study.

14. Hisham Shady N, Youssif KA, Sayed AM, Belbahri L, Oszako T, Hassan HM, Abdelmohsen UR. Sterols and triterpenes: Antiviral potential supported by in-silico analysis. Plants. 2020 Dec 26;10(1):41.

15. Shah A, Patel V, Parmar B. Discovery of some antiviral natural products to fight against novel coronavirus (SARS-CoV-2) using an in silico approach. Combinatorial chemistry & high throughput screening. 2021 Sep 1;24(8):1271-80.

16. Jain J, Kumari A, Somvanshi P, Grover A, Pai S, Sunil S. In silico analysis of natural compounds targeting structural and nonstructural proteins of chikungunya virus. F1000Research. 2017;6.

17. Singh S, Sk MF, Sonawane A, Kar P, Sadhukhan S. Plant-derived natural polyphenols as potential antiviral drugs against SARS-CoV-2 via RNA- dependent RNA polymerase (RdRp) inhibition: an in-silico analysis. Journal of Biomolecular Structure and Dynamics. 2021 Nov 2;39(16):6249-64.

18. Gurung AB, Ali MA, Lee J, Farah MA, Al-Anazi KM. Unravelling lead antiviral phytochemicals for the inhibition of SARS-CoV-2 Mpro enzyme through in silico approach. Life sciences. 2020 Aug 15;255:117831.

19. Mishra A, Pathak Y, Kumar A, Mishra SK, Tripathi V. Natural compounds as potential inhibitors of SARS-CoV-2 main protease: An: in-silico: study. Asian Pacific Journal of Tropical Biomedicine. 2021 Apr 1;11(4):155-63.

20. Liao, J., Wang, Q., Wu, F., & Huang, Z. (2022). In Silico Methods for Identification of Potential Active Sites of Therapeutic Targets. *Molecules (Basel, Switzerland)*, *27*(20), 7103. https://doi.org/10.3390/molecules27207103

21. Gupta SS, Kumar A, Shankar R, Sharma U. In silico approach for identifying natural lead molecules against SARS-COV-2. Journal of molecular graphics and modelling. 2021 Jul 1;106:107916.

22. Rathinavel T, Thangaswamy S, Ammashi S, Kumarasamy S. Virtual screening of COVID-19 drug from three Indian traditional medicinal plants through in silico approach. Res J Biotechnol. 2020 Oct;15(10):124-40.

23. Abdolmaleki S, Ganjalikhany MR. Binding affinity optimization and structural evaluation of designed antibodies against PD-1 and PD-L1 as critical immune checkpoints involved in cancer treatment.

24. Imran Kazmi, Fahad A. Al-Abbasi, Shareefa A. AlGhamdi, Amira M. Alghamdi et al. "Influence of rosiridin on streptozotocininduced diabetes in rodents through endogenous antioxidants-inflammatory cytokines pathway and molecular docking study" , Journal of Biomolecular Structure and Dynamics, 2023

25. Shaw DE, Maragakis P, Lindorff-Larsen K, Piana S, Dror RO, Eastwood MP, Bank JA, Jumper JM, Salmon JK, Shan Y, Wriggers W. Atomic-level characterization of the structural dynamics of proteins. *Science* **330:** 341–346 (2010).

26. Chaturvedi, M., Nagre, K.T., &Yadav, J.P. (2021). In silico approach for identification of natural compounds as potential COVID 19 main protease (Mpro) inhibitors. *VirusDisease, 32*, 325 - 329.

27. Abdolmaleki S, Ganjalikhany MR. Binding affinity optimization and structural evaluation of designed antibodies against PD-1 and PD-L1 as critical immune checkpoints involved in cancer treatment.

28. 28 KJ, Chow DE, Xu H, Dror RO, Eastwood MP, Gregersen BA, Klepeis JL, Kolossvary I, Moraes MA, Sacerdoti FD, Salmon JK. Scalable algorithms for molecular dynamics simulations on commodity clusters. InSC'06: Proceedings of the 2006 ACM/IEEE Conference on Supercomputing 2006 Nov 11 (pp. 43-43). IEEE.

29. Chow E, Rendleman CA, 28 KJ, Dror RO, Hughes DH, Gullingsrud J, Sacerdoti FD, Shaw DE. Desmond performance on a cluster of multicore processors. DE Shaw Research Technical Report DESRES/TR--2008-01. 2008 Jul 28.

30. Shivakumar, D., Williams, J., Wu, Y., Damm, W., Shelley, J., & Sherman, W. Prediction of Absolute Solvation Free Energies using Molecular Dynamics Free Energy Perturbation and the OPLS Force Field. Journal of Chemical Theory and Computation, (2010). 6(5), 1509–1519. doi:10.1021/ct900587b

31. Jorgensen, W. L., Chandrasekhar, J., Madura, J. D., Impey, R. W., & Klein, M. L. Comparison of simple potential functions for simulating liquid water. The Journal of Chemical Physics, (1983). 79(2), 926–935. doi:10.1063/1.445869

32. Martyna, G. J., Tobias, D. J. & Klein, M. L. Constant pressure molecular dynamics algorithms. J. Chem. Phys. (1994). 101: 4177–4189. doi:10.1063/1.467468

33. Martyna, G. J., M. L. Klein, and M. Tuckerman. Nose-Hoover chains-the canonical ensemble via continuous dynamics. J. Chem. Phys. (1992). 97:2635–2643. doi:10.1063/1.463940

34. Toukmaji AY, Board Jr JA. Ewald summation techniques in perspective: a survey. Computer physics communications. 1996 Jun 1;95(2-3):73-92.

35. Joshi T, Sharma P, Mathpal S, Pundir H, Bhatt V, Chandra S. In silico screening of natural compounds against COVID-19 by targeting Mpro and ACE2 using molecular docking. European Review for Medical & Pharmacological Sciences. 2020 Apr 15;24(8).